Study of the transport pathways in the African upper troposphere during the monsoon season based upon the assimilation of spaceborne CO observations in a CTM

Brice Barret, P. Ricaud, C. Mari, Jean-Luc Attié, N. Bousserez, B. Josse, E. Le Flochmoen, N.J. Livesey, S. Massart, V.H. Peuch, et al.

Atmos. Chem. Phys., 8, 3231–3246, 2008
www.atmos-chem-phys.net/8/3231/2008/

Atmospheric Chemistry and Physics

Transport pathways of CO in the African upper troposphere during the monsoon season: a study based upon the assimilation of spaceborne observations

B. Barret[1,2], P. Ricaud[1,2], C. Mari[1,2], J.-L. Attié[1,2], N. Bousserez[1,2], B. Josse[3], E. Le Flochmoën[1,2], N. J. Livesey[5], S. Massart[4], V.-H. Peuch[3], A. Piacentini[4], B. Sauvage[1,2], V. Thouret[1,2], and J.-P. Cammas[1,2]

[1]Université de Toulouse, Laboratoire d'Aérologie, Toulouse, France
[2]CNRS UMR 5560, Toulouse, France
[3]CNRM-GAME, Météo-France and CNRS URA 1357, Toulouse, France
[4]CERFACS, Toulouse, France
[5]Jet Propulsion Laboratory, California Institute of Technology, Pasadena, CA, USA

Received: 2 January 2008 – Published in Atmos. Chem. Phys. Discuss.: 13 February 2008
Revised: 7 May 2008 – Accepted: 2 June 2008 – Published: 26 June 2008

Abstract. The transport pathways of carbon monoxide (CO) in the African Upper Troposphere (UT) during the West African Monsoon (WAM) is investigated through the assimilation of CO observations by the Aura Microwave Limb Sounder (MLS) in the MOCAGE Chemistry Transport Model (CTM). The assimilation setup, based on a 3-D First Guess at Assimilation Time (3-D-FGAT) variational method is described. Comparisons between the assimilated CO fields and in situ airborne observations from the MOZAIC program between Europe and both Southern Africa and Southeast Asia show an overall good agreement around the lowermost pressure level sampled by MLS (∼215 hPa). The 4-D assimilated fields averaged over the month of July 2006 have been used to determine the main dynamical processes responsible for the transport of CO in the African UT. The studied period corresponds to the second AMMA (African Monsoon Multidisciplinary Analyses) aircraft campaign. At 220 hPa, the CO distribution is characterized by a latitudinal maximum around 5° N mostly driven by convective uplift of air masses impacted by biomass burning from Southern Africa, uplifted within the WAM region and vented predominantly southward by the upper branch of the winter hemisphere Hadley cell. Above 150 hPa, the African CO distribution is characterized by a broad maximum over northern Africa. This maximum is mostly controlled by the large scale UT circulation driven by the Asian Summer Monsoon (ASM) and characterized by the Asian Monsoon Anticyclone (AMA) centered at 30° N and the Tropical Easterly Jet (TEJ) on the southern flank of the anticyclone. Asian pollution uplifted to the UT over large region of Southeast Asia is trapped within the AMA and transported by the anticyclonic circulation over Northeast Africa. South of the AMA, the TEJ is responsible for the tranport of CO-enriched air masses from India and Southeast Asia over Africa. Using the high time resolution provided by the 4-D assimilated fields, we give evidence that the variability of the African CO distribution above 150 hPa and north of the WAM region is mainly driven by the synoptic dynamical variability of both the AMA and the TEJ.

Correspondence to: B. Barret
(barp@aero.obs-mip.fr)

1 Introduction

Carbon Monoxide (CO) plays an important role in tropospheric chemistry. It is an atmospheric pollutant produced by incomplete combustion processes (industries, transport, biomass burning (BB), (see Holloway et al., 2000, for a complete review). It affects both climate change, as an ozone (O_3) precursor (Daniel and Solomon, 1998), and the tropospheric oxidizing capacity as the main sink of the hydroxyl radical (OH) (Thompson, 1992). Furthermore, with a lifetime of 1–2 months in the troposphere, CO is an excellent tracer of polluted air masses. Fast economic growth in industrialised Asia have led to a fast increase of CO (Stavrakou and Muller, 2006) and other O_3 precursors such as nitrogen dioxide (NO_2) (Richter et al., 2005) and Volatile Organic Compounds (Fu et al., 2006) in the troposphere. Most of the state of the art Chemistry Transport Models (CTM's) underestimate tropospheric CO in the Norhern Hemisphere (NH)

Published by Copernicus Publications on behalf of the European Geosciences Union.

probably because of an underestimation of CO emissions from fossil fuel burning in east Asia (Shindell et al., 2006). Airborne and spaceborne observations of tropospheric CO have been used extensively to study intercontinental transport of pollution in the lower and free troposphere (Stohl et al., 2002; Duncan et al., 2004; Liang et al., 2007). Until recently, spaceborne CO observations were based on nadir viewing sensor in the infrared mostly sensitive to the free troposphere (Deeter et al., 2003; McMillan et al., 2005; Barret et al., 2005; Rinsland et al., 2006). Since August 2004, the Microwave Limb Sounder (MLS) onboard the Aura satellite provides unprecedented information about the global Upper Troposphere-Lower Stratosphere (UTLS) CO distribution (Filipiak et al., 2005; Livesey et al., 2008). These observations have allowed a better understanding of the CO transport processes in the UTLS (Li et al., 2005; Fu et al., 2006; Park et al., 2007).

The North African/Eastern Mediterranean UT is a crossroad impacted by transport processes on synoptic to seasonal timescales and on regional to intercontinental spatial scales. On seasonal scales, transport in the African UT is driven by the Hadley meridional circulation which is more intense in the winter Hemisphere. This circulation is characterized by a rising branch in the Inter Tropical Convergence Zone (ITCZ), poleward horizontal transport aloft and a sinking branch equatorward of the Suptropical Westerly Jets (SWJ). Sauvage et al. (2007a) studied the meridional gradients of O_3 in the African UT, observed by in-situ airborne measurements provided by the MOZAIC program. They put to the forth the impact of uplift of boundary layer O_3-poor air masses within the ITCZ followed by photochemical production of O_3 by O_3 precursors produced by lightnings or originating from the surface, within the upper level branches of the Hadley circulation. In particular, during the NH monsoon season in Africa, O_3 precursors emitted by BB south of the ITCZ and further transported to the ITCZ (Sauvage et al., 2005, 2007b; Mari et al., 2007) are likely to play an important role upon the African UT composition. Sauvage et al. (2007a) have also mentioned a possible impact of meridional transport by the northward flow on the western flank of the Asian Monsoon Anticyclone (AMA), that dominates the UT circulation in the Northern Hemispehere during the summer monsoon (Hoskins and Rodwell, 1995; Park et al., 2007), over the UT African O_3 distribution. Saunois et al. (2008) have used an idealized 2-D model to reproduce the O_3, water vapor (H_2O) and carbon monoxide (CO) meridional gradients in the African UT. Both studies give evidence of the Hadley circulation control upon the UT meridional O_3 gradient over Africa. However, large uncertainties remain concerning the impact of zonal transport from Asia upon the African UT composition.

In particular, during boreal summer, the African and the Asian UT are strongly connected through synoptic variations of the AMA centered at 30° N (Popovic and Plumb, 2001; Randel and Park, 2006) and fast horizontal transport by the strong westward winds of the Tropical Easterly Jet (TEJ) on the southern flank of the AMA (Sathiyamoorthy et al., 2007). Some evidence of the importance of zonal transport upon African tropospheric O_3 has been given in (Chatfield et al., 2004). Based on SHADOZ O_3 soundings, spaceborne tropospheric O_3 columns and trajectories calculations, they link the South Atlantic O_3 maximum to middle tropospheric westward transport of polluted air masses from the Indian Ocean over Africa to the Southern Tropical Atlantic during boreal spring. Li et al. (2001) have studied the origin of a summer tropospheric ozone maximum over the Middle East simulated with the GEOS-Chem CTM in agreement with observed O_3 vertical profiles. They found that O_3 photochemically produced in the Eastern and Southern Asian UT and transported westward by the TEJ accounts for 65% of the UT O_3 supply over the Middle East. In their study about the pollution crossroads over the Mediterranean, Lelieveld et al. (2002) have shown that Asian pollution uplifted by convection within the Asian Summer Monsoon (ASM) region can be transported westward over Africa and subsequently northward to the Eastern Mediterranean by the anticyclonic flow on the western flank of the AMA. This transport pathway contributes significantly to the enhanced CO concentrations observed over the Eastern Mediterranean in the UTLS. Evidence of this transport pathway has been further highlighted by (Scheeren et al., 2003) who have identified a BB plume originating in South Asia in the eastern Mediterranean UT, based on aircraft in situ chemical observations and backtrajectory analyses.

The aforementioned studies have given evidence of the strong impact of both Asian emissions through transport by the AMA during the NH monsoon season and African emissions through the Hadley circulation upon the African UT composition. The objective of our study is to address the main transport pathways of chemical species in the African UT and particularly to further discriminate the influence of these two transport pathways during the NH monsoon season. In order to achieve our goal, we have combined chemistry transport modeling and CO spaceborne observations from the limb viewing Aura/MLS through data assimilation. Assimilation of spaceborne chemical data in a CTM allows constraining the distribution of observed species while meteorological analyses give a realistic dynamical forcing. Therefore, the assimilation provides 4-D fields that are best suited to address transport processes and budget analyses (Pradier et al., 2006). Furthermore, the assimilated fields allow us to study variations of the transport processes on synoptic timescales (down to 6 h) while spaceborne observations from a limb sounder require averaging over several days to provide useful information. In this study we use the MOCAGE-PALM assimilation system to constrain the CO UTLS fields in the MOCAGE CTM with MLS observations for the month of July 2006. In the following, we will refer to our assimilation setup as MOCAGE-MLS. Both models and spaceborne observations need high quality independent

observations to be validated. The MOZAIC program has provided observations of the tropical UT composition (CO and O_3) for several years and particularly for the period of interest in this study which corresponds to the second phase of the AMMA (African Monsoon Multidisciplinary Analyses) airborne experiment Redelsperger et al., 2006; Mari et al., 2005; Lebel et al., 2007[1]. We have used those data to evaluate the MOCAGE model and the MOCAGE-MLS assimilation system.

Our paper is organized as follows. Section 2 is dedicated to the description of the whole assimilation setup covering the Aura/MLS CO observations in the UTLS, the MOCAGE CTM and the MOCAGE-MLS assimilation system. The validation of the assimilated fields based on MOZAIC aircraft in situ CO observations is discussed in Sect. 3. Section 4 is dedicated to the discussion of the July 2006 monthly mean CO UT distributions and to the main transport pathways of CO in the African UT. Section 5 provides an analysis of the variability of the UT CO distribution over Africa and of the dynamical processes responsible for this variability. Finally, summary and conclusions of the study are presented in Sect. 6.

2 The Assimilation of MLS CO data in the MOCAGE-PALM system

In this section we describe the three elements we have employed to perform the assimilation of Aura/MLS observations. First, we discuss the Aura/MLS CO observations in the UTLS and the way we have actually utilized them. Second, the main characteristics of the MOCAGE CTM with the direct simulation we have performed are exposed. Finally we give the main details of both the assimilation setup and the assimilation performances.

2.1 Aura/MLS observations of CO in the UTLS

The MLS instrument has been flying onboard the Aura satellite in a sun-synchronous polar orbit since August 2004. Vertical profiles of 17 atmospheric parameters are retrieved from the millimeter and sub-millimeter thermal emission measured at the atmospheric limb (Waters et al., 2006). The latest MLS CO observations we use in this study (V2.2) are described in Pumphrey et al. (2007). One of the most interesting features of MLS is its ability to measure CO and other constituents in the UTLS where retrievals are made at 4 levels, namely 215, 147, 100 and 68 hPa. Furthermore, the relatively low sensitivity of measurements in the millimeter and sub-millimeter domain to high humidity and clouds allows MLS to provide a good spatial coverage in the tropical UT. MLS CO data in the UTLS have a 4 to 5 km vertical resolution, a 500 to 600 km along-track resolution and a precision of ∼20 ppbv (Livesey et al., 2008). Livesey et al. (2008) have made detailed characterization and validation of MLS CO and O_3 data in the UTLS. The Aura/MLS CO observations used in our assimilation system have been screened according to their recommendations. For the 147, 100 and 68 hPa MLS retrieval levels, Livesey et al. (2008) estimate a scaling uncertainty of 30%. Comparing MLS CO and MOZAIC in situ airborne CO observations at northern mid-latitude they show that MLS CO at 215 hPa is roughly a factor of 2 too high and they deduce a scaling uncertainty of ∼100% at that level. In their validation studies, Clerbaux et al. (2008) and Pumphrey et al. (2007) have compared CO profiles measured by the ACE-FTS (Bernath et al., 2005) and Aura/MLS instruments. They both show that MLS is biased high in the UT with the highest relative difference (∼100%) found around 12 km and that the bias is the lowest in the Lower Stratosphere (LS) around 18–20 km. On the basis of the validation studies aforementioned, our first concern regarding the assimilation of MLS CO data has been to find the best way to estimate the biases of these observations at the 4 UTLS retrieval levels within the scaling uncertainties described in Livesey et al. (2008). In order to achieve this task, we have used the ACE-FTS tropical CO climatology from Folkins et al. (2006a) (see their Fig. 12). Indeed, some limitations of the ACE-FTS sensor (e.g. limited number of profiles measured per day, high sensitivity to clouds and humidity, lower coverage of tropical versus polar latitudes) make a direct validation of our assimilated fields for a one month period at tropical latitudes rather difficult. In Table 1 we have reported the climatological values from ACE-FTS computed by Folkins et al. (2006a) and the mean tropical CO values from MLS at the 4 UTLS retrieval levels for the month of July 2006. As expected, the highest difference between the two instruments occurs at 215 hPa, with a MLS/ACE ratio of 1.62. Nevertheless this ratio is much lower than the value of 2.0 that has been estimated by the validation studies we have mentioned before. Comparisons between analyses performed with the MLS data at 215 hPa rescaled by factors ranging from (1.0) to (1/2.0) and MOZAIC aircraft in situ observations have led us to use a slightly higher value (1/1.7) to adjust the MLS observations at 215 hPa. The results of the final comparison, showing an agreement within 5% between analyses and MOZAIC data, are given in Sect. 3. At 147 hPa, the agreement between the ACE-FTS climatology and the mean MLS tropical value is rather good, and we have rescaled the MLS observations by a factor of 1/1.05. The 100 hPa MLS tropical CO values are biased high by 23% relative to the ACE-FTS climatology. Therefore, MLS partly misses the steep vertical gradient observed in the tropics from 14.5 km to the LS by ACE-FTS and confirmed by various aircraft campaigns (Folkins et al., 2006a). The adjustment of the MLS CO observations by 1/1.2 at 100 hPa will compensate this bias. At

[1] Lebel, T., Parker, D. J., Bourles, B., Flamant, C., Marticorena, B., Peugeot, C., Gaye, A., Haywood, J., Mougin, E., Polcher, J., Redelsperger, J.-L., and Thorncroft, C. D.: The AMMA field campaigns: Multiscale and multidisciplinary observations in the West African region, Ann. Geophys., submitted, 2007.

Table 1. CO tropical (20° S–20° N) mixing ratios in the UTLS and scaling factors applied to the Aura-MLS observations. In the tropics, the 4 altitudes given in this table roughly correspond to the 4 UTLS retrieval pressure levels of MLS (215, 147, 100 and 68 hPa). The ACE climatological values are from Folkins et al. (2006).

Altitude	Tropical CO vmr				Scaling factor	
(km)	ACE	MLS	MOCAGE	MOCAGE-MLS	MLS/ACE	Applied factor
12.5	90.	146.	81.	86.	1.62	1.7
14.5	85.	89.	74.	83.	1.05	1.05
16.5	55.	68.	59.	58.	1.23	1.2
18.5	30.	29.	31.	28.	0.97	1.0

68 hPa, the mean MLS tropical value is close to the ACE-FTS climatology, in agreement with Pumphrey et al. (2007) and Clerbaux et al. (2008) and we have kept the original values.

2.2 Model description

MOCAGE is the global CTM developed at the CNRM (Centre National de Recherches Meteorologiques) of Meteo-France (Bousserez et al., 2007; Teyssedre et al., 2007; Ricaud et al., 2007). It provides numerical simulations of the interactions between dynamical, physical and chemical processes in the troposphere and the stratosphere. It uses a semi-lagrangian advection scheme to transport the species (Josse et al., 2004). The model is constrained with the European Center for Medium range Weather Forecast (ECMWF) 6-hourly meteorological analyses (horizontal winds, temperature, specific humidity, surface pressure). The vertical velocities are computed from the ECMWF horizontal wind fields by imposing the mass conservation law for each atmospheric column. The simulations are performed on a regular $2^\circ \times 2^\circ$ horizontal grid and on 47 hybrid (σ, P) levels from the surface up to 5 hPa. The vertical resolution typically varies from 40 to 400 m in the boundary layer (7 levels) and is about 800 m in the UTLS. The chemical scheme used is RACMOBUS, which combines the stratospheric scheme REPROBUS (Lefevre et al., 1994) and the tropospheric scheme RACM (Stockwell et al., 1997). Convective processes are simulated with the scheme of Bechtold et al. (2001), and turbulent diffusion is calculated with the scheme by Louis (1979). For anthropogenic (including BB) sources, the model uses the emission inventory from Dentener et al. (2005) with a monthly or yearly time-resolution depending on the species. In particular, nitrogen oxides (NO_x), CO and Volatile Organic Compounds emissions from BB have a monthly time-resolution. The total CO surface emissions representative of year 2000 amounts to 1094 $Tg(CO)\,yr^{-1}$. We started our simulations on 1 January 2006 from a climatological initial field in order to have a 6 months spin-up before July 2006. In the following we will discuss results from a direct simulation with the MOCAGE CTM (control run) and from the assimilation of MLS CO observations with the MOCAGE-MLS system (assimilation run) for July 2006.

2.3 Assimilation setup

Data assimilation systems have been developed to tackle tropospheric chemistry and transport focusing on CO observations (see e.g. Lamarque et al., 2004; Yudin et al., 2004; Pradier et al., 2006). To our knowledge, the UTLS region has not yet been the subject of scientific studies based on spaceborne CO data assimilation while new limb sensors, such as Aura/MLS (Livesey et al., 2008) or Envisat/MIPAS (Raspollini et al., 2006) provide information about the UTLS composition. The sparse horizontal sampling of such limb sensors requires averaging over time periods ranging from several days to weeks in order to obtain global distributions useful for scientific purposes. However, the UTLS composition variability, driven by transport and chemistry processes on synoptic timescales cannot be captured by such averaging procedures. The coarse vertical resolution of UTLS spaceborne measurements does not allow to resolve processes with finer vertical scales typical of this atmospheric region. Furthermore, the lack of regular independent in situ observations in the tropical UTLS makes the validation of spaceborne observations particularly difficult in this region. Finally, as mentioned in the introduction, global CTM's have problems to reproduce the tropospheric composition and more particularly the CO tropospheric distribution (Shindell et al., 2006). Therefore, the goals of the assimilation of UTLS Aura/MLS CO data in the MOCAGE CTM presented in this study are manyfold: (i) to estimate the concentrations of CO at altitudes where they are not observed by MLS (ii) to fill in temporal and spatial gaps from the Aura/MLS CO measurements to enable the study of the processes responsible for the CO distribution variability on synoptic timescales (iii) to evaluate the representation of UTLS CO transport and chemistry processes in the MOCAGE CTM and (iv) to support the validation of the Aura/MLS CO observations. Our study is based on the assimilation of UTLS CO observations by the Aura/MLS sensor in the MOCAGE CTM with a 3-D-FGAT

(First Guess at Assimilation Time,) assimilation method driven by the PALM software developed at CERFACS (Buis et al., 2006; Massart et al. , 2005). This MOCAGE-PALM assimilation system has been tested for the assimilation of stratospheric O_3 within the framework of the Assimilation of Envisat Data (ASSET) project (Geer et al., 2006). The 3-D-FGAT method has the advantage to take the dynamics of the system into account to compute the difference between the model and all the observations located in a given temporal window (3 h in our case).

The assimilation consists in the iterative minimization of a cost function computed from the differences between the observations and the model background weighted by their respective covariance matrices. The choice of the observation and of the background covariance matrices is therefore important to reach the right balance between the background and the observations. We have assumed that the observations at the different retrieval levels were independent and we have therefore used a diagonal covariance matrix for the observation error. In order to spread assimilation increments spatially, horizontal background correlations are modelled using a generalized diffusion operator (Weaver and Courtier, 2001) with a scale-length of 4° and vertical background error correlations are modelled using an exponential law with a scale-length of ∼2 km (Massart et al., 2007). A quantitative criterion for the choices of the background and observations errors is the chi-square (χ^2) test. The normalised χ^2 is the ratio of the cost function to half the number of observations in the assimilation window. A value of χ^2 close to 1 indicates a good balance while a value higher (respectively lower) than 1 indicates an underestimation (respectively overestimation) of the observation or background error covariance matrices. We have performed assimilations with different choices of the background and observation errors in order to reach a χ^2 value close to 1. Satisfactory results have been achieved using a background error of 10% throughout the UTLS and observation errors from the MLS files (Livesey et al., 2008) scaled by 0.9. During the first day of the assimilation period, the χ^2 are of the order of 0.9 and after 2 days of assimilation the χ^2 remain stable within the range 0.65–0.75. While these values are lower than 1, indicating possible overestimations of the background or observation errors, we have chosen to decrease neither the background nor the observation errors. First, comparisons between CO from the control run and MOZAIC in situ data show that around 220 hPa, the model random error (15–20%) is larger than the 10% error we have prescribed for the model background. Second we prefer to keep the observation errors prescribed in the assimilation system close to the errors given in the MLS files because they are based on instrumental considerations (Livesey et al., 2008).

2.4 Assimilation results

In order to evaluate the CO fields from the control and the assimilation runs, we have first checked the consistency between the mean tropical CO volume mixing ratio (vmr) and the ACE-FTS climatology used to adjust the MLS observations in the UTLS. The results are given in Table 1. The model underestimates CO in the tropical UT by ∼10 ppbv while in the tropical LS, mean modelled CO vmr's are in good agreement with the ACE-FTS climatology. At the 3 MLS retrieval levels in the UT, the assimilation results in an improved agreement (within ∼4 ppbv) with the climatology. The CO fields from MLS, and from the control and assimilation runs, averaged over the period 5–31 July 2006 are shown in Fig. 1 in a large domain encompassing Africa and Asia. As expected, the assimilation results in a large improvement of the agreement relative to the observations. At the 3 lowermost UTLS levels, the correlation coefficients between model and observations are in the range 0.59–0.71 and 0.85–0.88 between assimilation and observations. At 215 and 147 hPa the mean low biases between the control run and both the MLS observations and the assimilation run are clearly visible in Fig. 1. On a more regional scale, important discrepancies between the control run and MLS/assimilation run are occuring around the ASM and WAM regions. At 215 and 147 hPa over Asia, MOCAGE is biased low relative to MLS, but the structure of the CO distribution is in rather good agreement with the structure detected by MLS. Such a low bias can be attributed to the emission inventory used in MOCAGE that did not take the fast industrial growth of Southeast Asia and particularly China in the last years (Richter et al., 2005; Stavrakou and Muller, 2006; Fu et al., 2006) into account. Such a problem has been reported by Shindell et al. (2006) for most of the state of the art global CTM's. At 100 hPa, the CO enhanced concentrations within the AMA observed by MLS and reproduced by the assimilation run are not visible with the control run. A low bias in the Asian CO emissions may also explain this low bias in the CO distribution. Nevertheless, the difference of structure in the CO observed and modeled distributions at 100 hPa most likely points to a problem related to the model dynamics (too weak monsoon circulation) and/or the convective parametrization in this region. At 215 hPa over the WAM, the model overestimates the CO concentrations relative to the MLS observations. Important quantities of the CO uplifted to that level by WAM convection comes from BB in Southern Africa (Sauvage et al., 2005, 2007b; Mari et al., 2007). Therefore, the discrepancy between the control run and MLS most likely points to an overestimation of the climatological African BB emissions in the MOCAGE inventory.

In order to evaluate our assimilation system and its time evolution, we have computed the daily mean differences between observations and assimilated fields, named Observations minus Analyses (OmA) and between the observations and the fields simulated by the control run that we name

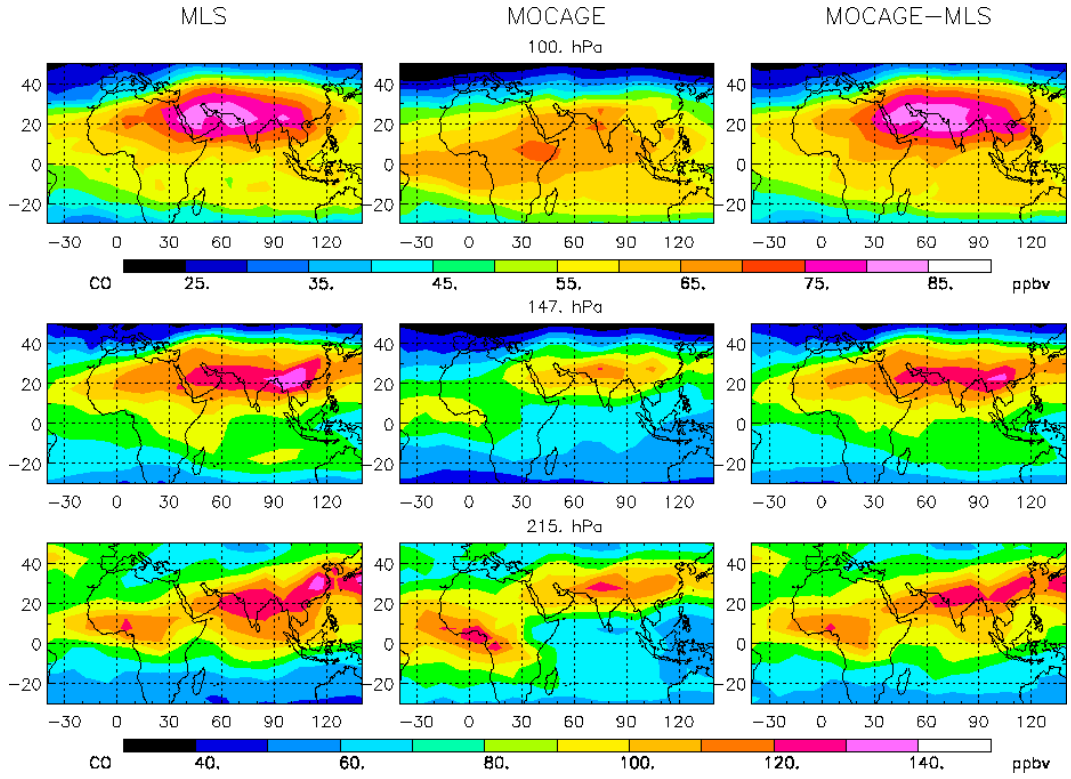

Fig. 1. CO fields at the 3 MLS retrieval levels in the UTLS averaged over the period 5–31 July 2006: (top panels) 100 hPa, (middle panels) 147 hPa and (bottom panels) 215 hPa. From left to right: MLS observations, simulated fields with the MOCAGE model and assimilated fields with the MOCAGE-MLS assimilation system.

Observations minus Direct (OmD). The OmA and OmD are displayed in Fig. 2 for 100, 147 and 215 hPa for a global domain between 40° S and 40° N and for Asia from 10° N to 40° N and 60° E to 110° E. Asia has been chosen as a test region because the highest differences between the model and the MLS observations occur over Asia (Fig. 1). Over both domains and for the three pressure levels, the OmA is converging to an almost steady value within 1 to 3 days. Over the global domain the OmA remain within the (−2)−2 ppbv range while the OmD is in the range 2–5, 9–12 and (−1)–(−2) ppbv at 215, 147, and 100 hPa, respectively. Over Asia, OmD's are higher and display more variability than over the global domain with typical values between 10 and 20 ppbv. However, after 3 days of assimilation, the OmA's remain within the (−5)−5 ppbv range at the 3 pressure levels. Therefore, we can use the assimilated fields starting conservatively 6 days after the beginning of the assimilation period (5 July) relying on an agreement within 5 ppbv with the MLS observations.

3 Validation of the assimilated fields

In this section, we first make use of the MOZAIC data to validate the MOCAGE-MLS assimilated distributions. These observations are the only available regular UTLS CO in situ observations performed during our study period. Nevertheless, as they are carried out onboard commercial aircrafts, they only provide information about the lowermost part of the vertical domain under study, namely below ∼200 hPa. Therefore, we discuss the method we have used to rescale the MLS data and its possible impact on the vertical structure of the MOCAGE-MLS assimilated distributions.

3.1 MOZAIC observations

As part of the MOZAIC program, in-situ measurements of CO and O_3 have been performed daily from Windhoek (22.5° S, 17.5° E, Namibia) to Frankfurt (50° N, 8.6° E, Germany) since December 2005 with instruments onboard a commercial Air-Namibia aircraft. From 5 to 31 July, we have used data from the 27 daily flights. MOZAIC CO and O_3 regular measurements are also available from Austrian-Airlines commercial flights from Vienna (48.1° N, 16.2° E, Austria) to Bangkok (13.4° N, 100.3° E, Thailand) since beginning

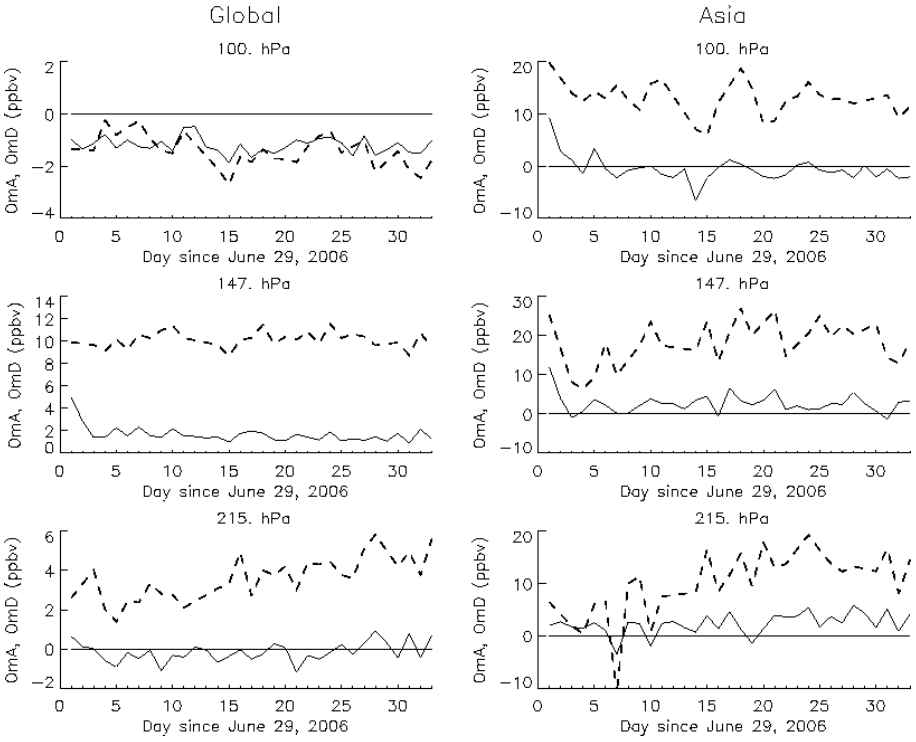

Fig. 2. Time evolution of the differences between the MLS observations and (solid lines) the MOCAGE-MLS analyses (OmA) and (dashed lines) the MOCAGE dircet simulations (OmD) at the (top panels) 100, (middle panels) 147 and (bottom panels) 215 hPa pressure levels. The OmA and OmD are computed for (left panels) a global domain between 40° S and 40° N and for (right panels) Asia from 10° N to 40° N and 60° E to 110° E.

of 2006. For our study period (5–31 July 2006), we have gathered data from 13 Austrian-Airlines flights to Bangkok. MOZAIC measurements carried out with a 30 s response time and with a reported precision of ∼5 ppbv for CO (Nedelec et al., 2003) have been averaged in 1 mn time bins. For the comparisons, outputs from the control and assimilation runs have been interpolated to the 1 mn averaged observation times and locations. We have selected data recorded with a flight pressure level lower than 250 hPa in order to have enough data for statistical comparisons and to be close enough to the lowermost level (215 hPa) of the MLS CO observations used in the MOCAGE-MLS assimilation system.

3.2 Validation results

The comparisons between the MOZAIC CO observations and the outputs from the control and assimilation runs are displayed in Fig. 3 for the Air-Namibia data and in Fig. 4 for the Austrian-Airlines data. The data have been averaged over the period 5–31 July 2006 in 2° latitude bins for Air-Namibia and in 2° longitude bins for Austrian-Airlines. In both cases the average biases between the modelled and assimilated CO fields and the MOZAIC observations are positive and not exceeding 4 ppbv or 5%. The good overall agreement between

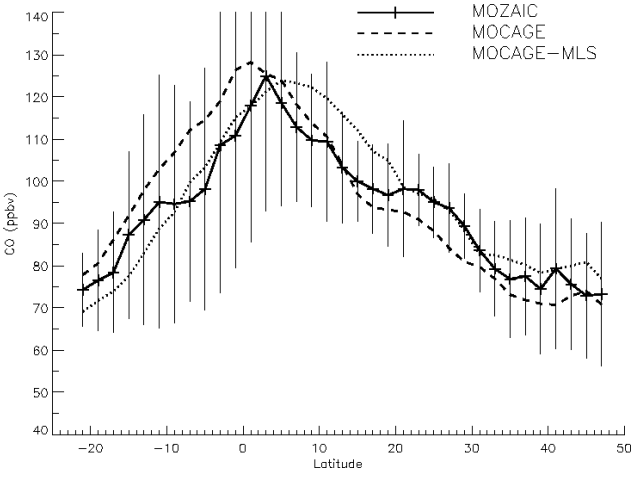

Fig. 3. Windhoek (22° S–17° E)-Frankfurt (50° N–9° E) CO latitudinal transects above 250 hPa: (crosses and solid line) MOZAIC observations, (dashed line) MOCAGE simulations and (dotted line) MOCAGE-MLS assimilated fields. Data have been averaged over 5–31 July 2006 in 2° latitude bins. The vertical error bars represents the 1σ MOZAIC variability.

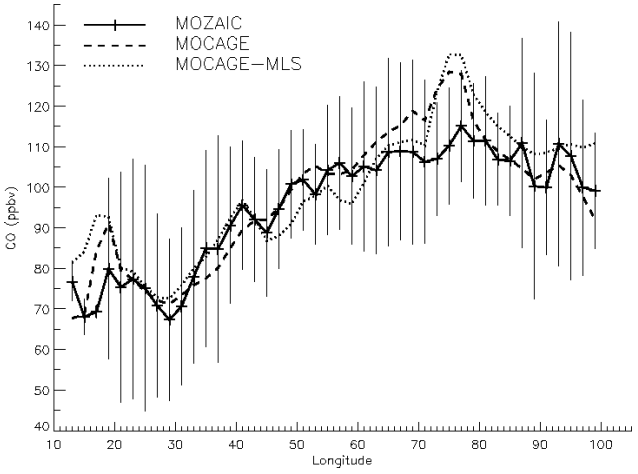

Fig. 4. Same as Fig. 3 for the Vienna (48° N–16° E)-Bangkok (13° N–100° E) CO longitudinal transects.

MOZAIC and the assimilated fields was expected since the scaling factor applied to the MLS observations at 215 hPa was partly chosen from comparisons between MOZAIC data and assimilation tests (Sect. 2.1). The control and the assimilation runs reproduce the observed CO meridional gradient correctly (Fig. 3) with a sharp increase north of 22° S, maxima between roughly the Equator and 5° N, and globally decreasing gradients from Equator-5° N to 35° N. Discrepancies between the control run and the MOZAIC observations are found between 10° S and the equator where MOCAGE overestimates CO by 10–15 ppbv and north of 20° N where the model underestimates the in situ observations by less than 10 ppbv. The assimilation run displays a very good agreement with MOZAIC between 10° S and 5° N. Between 5° N and 20° N, the assimilation overestimates CO by ∼10 ppbv. The differences between the control and the assimilation runs indicates that this overestimation probably comes from a bias in the MLS observations. The agreement between MOZAIC and the assimilation run is again excellent from 20° N to 50° N. The longitudinal transect from Germany to Thailand from MOZAIC, and from the control and assimilation runs are in very good agreement (Fig. 4). Both the model and the assimilation system are able to reproduce the south-eastward increase of UT CO. The only noticeable discrepancy is an overestimation of the CO vmr's by up to 20 ppbv between 70° E and 85° E by both the model and the assimilation system relative to the MOZAIC data. The consistency between the model and assimilation suggests a bias from the model rather than from the MLS observations. Furthermore for the 7 days with MOZAIC observations below 250 hPa in this region, the MLS sampling is relatively poor and consequently the spaceborne observations do not constrain the model enough to correct the bias.

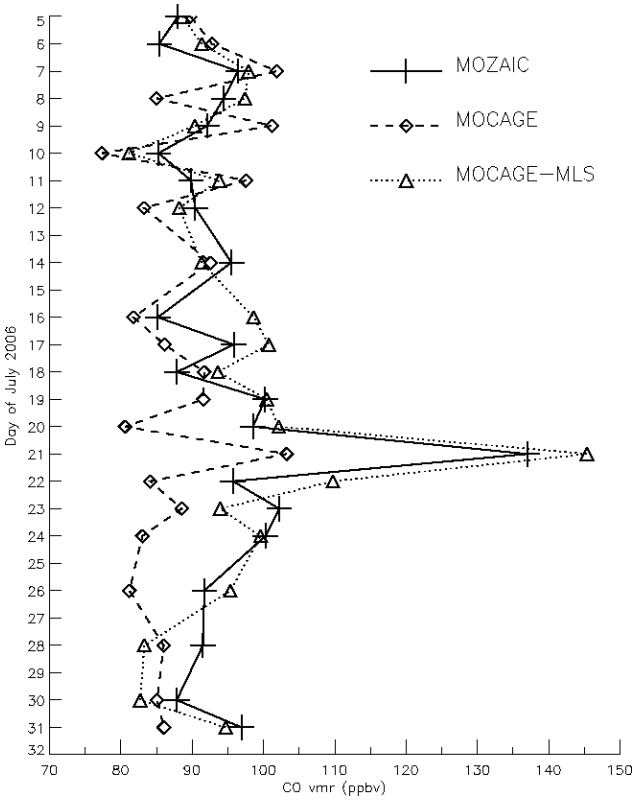

Fig. 5. Time evolution of CO in the 20° N–30° N latitudinal band above 250 hPa over Africa: (crosses and solid line) MOZAIC Air-Namibia observations, (dashed line) MOCAGE simulations and (dotted line) MOCAGE-MLS assimilated fields.

An important aspect of the assimilation of spaceborne data is its ability to produce 4-D fields enabling to follow processes occuring on synoptic timescales not fully captured by the observations. Thanks to their daily frequency, the MOZAIC Air-Namibia program provides a very good set of data to evaluate the ability of our assimilation system to follow the CO daily variability over Africa. Figure 5 presents the time evolution of the mean daily CO concentration between 20° N and 30° N and above the 250 hPa level sampled along the aircraft flight track. Before 18 July and after 27 July, the model and the assimilation system reproduce correctly the measured CO variations characterized by oscillations within the 80–95 ppbv range. The enhanced CO concentrations observed by MOZAIC from 19 to 26 July and the sharp peak characterized by CO concentrations exceeding the background mean value by more than 50 ppbv observed on 21 July are far better reproduced by the assimilation system than by the model. From our comparisons with the MOZAIC observations we conclude that the assimilated CO distributions at the lowermost boundary of the assimilation region are satisfactory. The mean bias between the assimilated fields and the in situ observations is below 5%. The

main structures of the transects between Europe and Africa and between Europe and Southeast Asia are well reproduced by MOCAGE-MLS and the assimilation system is able to reproduce sporadic short events not simulated by the model.

3.3 Discussion of the MLS rescaling method

The annual cycle of UT tropical CO displays a minimum during boreal summer (JJA) (Folkins et al., 2006b). The climatology of Folkins et al. (2006a) we are using to rescale the MLS data is an annual climatology based on 2004–2005 ACE-FTS data. Therefore, our MOCAGE-MLS assimilated tropical distributions may be overestimated. In order to quantify this possible overestimation, we have computed an annual and a JJA CO climatology based on ACE-FTS data for years 2004 to 2007. It has to be noted that due to the sparse sampling of the ACE-FTS sensor in the tropics, less than 50 valid tropical profiles are measured per season for the full period. The annual climatology, based on about 200 tropical profiles, therefore provides a more robust representation of the CO vertical structure in the tropics than the JJA climatology. Furthermore, our annual climatology falls within 5% of the climatology of Folkins et al. (2006a) and further validates it. The absolute differences between the climatology of Folkins et al. (2006a) and our JJA climatology at 215, 150 and 100 hPa are respectively 11, 15 and 5 ppbv. Therefore, applying the JJA climatology to rescale the MLS data would not dramatically change the vertical structure of the MOCAGE-MLS distributions. The main effect would be a reduction of the sharp vertical gradient between 14.5 and 16.5 km from 15 to 10 ppbv/km. Furthermore, using the JJA climatology at 215 hPa would lead to require a factor (1/1.84) to rescale the MLS data and therefore to a 10% underestimation of the assimilated fields relative to the MOZAIC in situ observations. This difference, which indicates a possible low bias in the ACE-FTS data around 200 hPa, has further encouraged us to use the annual climatology of Folkins et al. (2006a) rather than our JJA climatology.

To conclude, the most important bias of MLS at the 215 hPa level has been successfully corrected using the ACE-FTS climatology and a slight adjustment with the MOZAIC data (Sects. 2.1 and 3.2). Furthermore, the use of the ACE-FTS annual climatology has allowed us to consistently correct the MLS biases along the vertical dimension from 215 hPa upwards.

4 Transport pathways of CO in the African UT

In this section, we discuss the main transport pathways in the African UT on a monthly scale based on July 2006 averaged fields from the assimilation run. The aim is to make an assessment of the relative impact of long range transport of pollution from Asia and of local African emissions upon the African UT CO distribution. The assimilation of MLS CO observations in the MOCAGE CTM has two important advantages to fulfill this task: (i) relative to the sparse MLS observations, the assimilated CO fields have a full 4-D coverage that allows us to study the dynamical tendencies in combinations with the ECMWF dynamical analyses (ii) relative to the MOCAGE CTM, the constraint brought by the MLS observations allows us to correct biases in the model and to provide more realistic CO distributions at high spatial and temporal resolution (Sect. 2.4). Numerous recent studies have pointed to the strong uplift of boundary layer polluted air from India Southeast Asia and South China to the Asian UT during the ASM (Li et al., 2001; Lelieveld et al., 2002; Li et al., 2005; Fu et al., 2006; Park et al., 2007; Berthet et al., 2007). Based on simulations from the GEOS-Chem CTM, Li et al. (2005) explain this uplift by (i) enhanced convection resulting from wind convergence in southwest China and, (ii) orographic lifting of the southwesterly flow from Bangladesh and Northeast India over the southern slope of the Himalayas. Using trajectory calculations Berthet et al. (2007) have also highlighted the potential of South China, Indian subcontinent as a source of pollutants transported from the boundary layer to the tropopause region and LS in summer. The mean CO distributions at 100, 150 and 220 hPa from the assimilation run together with the horizontal winds, the Outgoing Longwave Radiation (OLR) 200 and 220 W/m^2 characterizing deep convection (Park et al., 2007) and the dynamical tropopause contours superimposed and averaged over the period 5–31 July 2006 are displayed in Fig. 6. At 220 hPa above Asia, the highest CO concentrations from MOCAGE-MLS are located between 20° N and 30° N and more specifically over Northeast India/Nepal and over Southwest China (Fig. 6c) confirming the transport pathways highlighted by Li et al. (2005). From spaceborne observations and back-trajectories calculations, Fu et al. (2006) argue that moist convection driven by enhanced surface heating over the Tibetan Plateau is deeper and detrains more water vapor and CO at the tropopause level than convection over the ASM region. As already described by Park et al. (2007), the OLR are lower over the ASM region (see the 200 W/m^2 OLR contour in Fig. 6c) than over the Tibetan Plateau. Furthermore, no elevated CO concentrations are noticeable right over the the Tibetan Plateau at 220 hPa (Fig. 6c). Our results tend to mitigate the possible impact of Tibetan Plateau convection as a predominant transport pathway to the Asian UT. The TEJ centered at 10° N and blowing from India and the Indian Ocean to Africa is responsible for the high CO concentrations over the Arabic sea and the Arabic peninsula. This inflow of CO-enriched air masses from Asia is consistent with the results of Li et al. (2001) concerning the major role of UT westward transport of O_3 from Asia to sustain the Middle East tropospheric ozone maximum in summer.

Over Asia during the ASM, the UT circulation is dominated by the AMA driven by diabatic heating in the ASM region (Hoskins and Rodwell, 1995; Park et al., 2007). The AMA is bounded by the Subtropical Westerly Jet on its

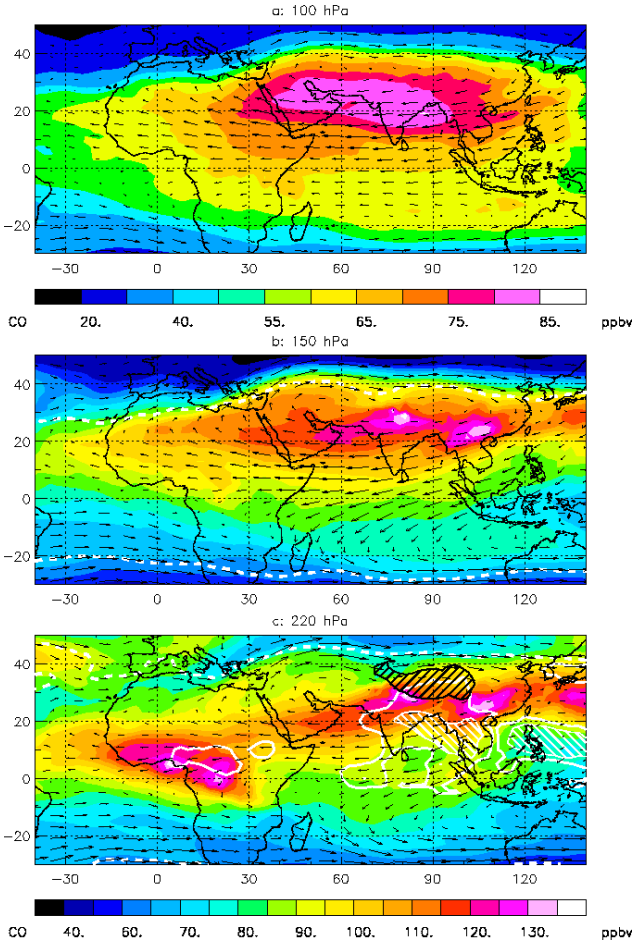

Fig. 6. CO assimilated fields averaged over the period 5–31 July 2006 at **(a)** 100 hPa, **(b)** 150 hPa and **(c)** 220 hPa. Superimposed are: (black arrows) the horizontal winds from the ECMWF operational analyses, (white dashed contour) the dynamical tropopause. In panel c: white contours indicate deep convection (OLR contours 220 and 200 W/m^2, with values below 200 hatched white), and Tibetan plateau is shown as black hatched area within black contour where surface altitude is greater than 3000 m. a.s.l.

northern flank (∼40° N) and by the TEJ on its southern flank (∼10° N) and is extending on average from 20° E to 120°E. Based on UT Aura/MLS observations at 150 hPa, Li et al. (2005) have highlighted the trapping of polluted air masses within the AMA. Using O_3 and H_2O tropospheric observations from the Atmospheric Infrared Sounder (AIRS), Randel and Park (2006) have also established that transient convective events were responsible for the vertical transport of H_2O enriched and O_3 poor air masses up to the UT (∼13 km), where the constituent anomalies are confined within the AMA. In a more recent study, Park et al. (2007) have taken advantage of a large range of UTLS spaceborne observations such as Aura/MLS CO, O_3 and H_2O, to establish that this behavior extends to the LS at 100 hPa. The CO distributions from MOCAGE-MLS at 150 and 100 hPa (Fig. 6a and b) confirm that polluted air masses are isolated within the AMA in the upper levels of the UT and in the LS. However, the uplift processes are still responsible for localized enhanced CO concentrations at 150 hPa, while the 100 hPa distribution is more homogeneous within the AMA highlighting slower uplift processes to the LS resulting in a better mixing of the air masses. At 220 hPa over Africa, the maximum values of CO (120 ppbv) are located around the WAM region, identified by low OLR (Fig. 6c). In order to highlight the dynamical processes that drive the UT CO distributions over Africa we have computed latitude-pressure cross-sections of CO mixing ratios (Fig. 7a) and of CO dynamical tendencies (Fig. 7b, c and d) based upon the ECMWF wind analyses and the 4-D CO assimilated fields for a zonal band encompassing Africa (20° W–30° E). The main contributor to the enhanced CO concentrations between 0° N and 12° N and below ∼180 hPa is convective uplift responsible for the injection of up to 45 ppbv of CO per day (Fig. 7d). During the WAM season, BB which occurs in Southern Africa from 20° S to the ITCZ around 5° S (Mari et al., 2007) is the main source of CO in Africa. In order to be uplifted to the UT by deep convection to produce the maximum CO concentrations in the WAM region displayed in Fig. 6c, BB emissions have to be transported to the ITCZ. Sauvage et al. (2005) and Sauvage et al. (2007b) point to a connection between southern regions impacted by BB and the WAM mid-troposphere through transport by the south-easterly trade winds above the monsoon layer. Mari et al. (2007) argue that air masses impacted by BB are transported out over the ocean by the southern hemispheric African Easterly Jet (AEJ-S) or toward the continental part of the ITCZ during the break phase of the AEJ-S. Below 180 hPa, CO deposited by vertical transport in the WAM region is vented primarily by southward advection within the southern Hadley cell, more intense than its northern counterpart, with negative tendencies in the range of 20–45 ppbv/day that compensate the uplift tendencies (Fig. 7b). This southward transport results in high concentrations of CO over Southern Africa down to 10° S at 220 hPa (Fig. 6c) confirmed by the MOZAIC observations (Fig. 3). North of the ITCZ, between 12° N and 20° N, zonal advection of polluted air masses by the TEJ blowing from India is the most important source of CO (Fig. 7c) to maintain the enhanced concentrations noticeable over Africa at 220 hPa (Fig. 6c). Nevertheless, the validation performed with the MOZAIC data showing an overestimation of ∼10 ppbv of CO by the assimilation run in that region (Sect. 3.2) makes us mitigate the impact of this zonal transport upon the CO distribution. Air masses impacted by African pollution and uplifted in the WAM region contribute much less to the CO budget north of the ITCZ because northward transport is predominant only north of the ITCZ (Fig. 7b). This result further highlights that the high bias observed between the control run and MOZAIC south of the CO maximum (∼3° N) over Africa (Sect. 3.2)

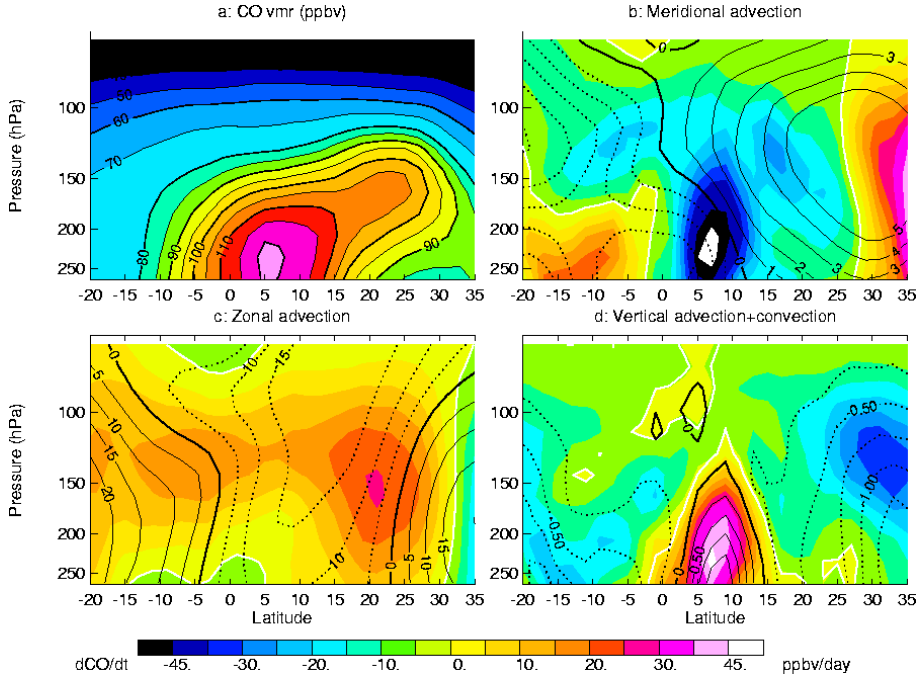

Fig. 7. Latitude-pressure cross sections over Africa (20° W–30° E) for **(a)** the CO distribution (ppbv) **(b)** the meridional advection tendency **(c)** the zonal advection tendency **(d)** the sum of the vertical advection and convective tendencies. The zero tendencies are materialized by white contours and the winds by black dotted (resp. solid) contours for (b) southward (resp. northward) (m/s), (c) westward (resp. eastward) (m/s), and (d) downward (resp. upward) (cm/s) winds. The thick solid contour corresponds to the zero wind speed.

is probably resulting from too strong African BB emissions during boreal summer in the model. North of 20° N, the TEJ splits over the Middle East and turns clockwise, bringing polluted air masses to the Eastern Mediterranean as described in Lelieveld et al. (2002). West of 20° E, a well-marked westerly flow brings clean oceanic air over Northern Africa. At 150 hPa, the African CO maximum concentrations (∼110 ppbv) are located over the Sahara around 25° N (Figs. 6b and 7a). This northward shift of the CO maximum is caused by three main processes. First, convection is weaker over the WAM than over the ASM region (see the 200 W/m^2 contour in Fig. 6c) (even though ASM convection is not responsible for the main transport of CO to the Asian UT as was discussed above). In the WAM region, positive upward tendencies are therefore much weaker at 150 hPa (∼10–15 ppbv/day) than at 220 hPa (Fig. 7d) and the CO concentrations do not exceed 105 ppbv. Second, the AMA circulation is stronger at 150 hPa than at 220 hPa and the CO enriched air masses originating from Asia that have been uplifted to the UT and trapped within the AMA are therefore transported over Northeast Africa. Finally, on the AMA southern flank (between 10° N and 25° N) the TEJ which is also stronger at 150 hPa than at 220 hPa, is responsible for the westward transport of polluted air masses from Asia to the African Atlantic coast. Both processes linked to the strong anticyclonic circulation over Asia result in maxima CO positive tendencies around 20 ppbv/day between 15° N and 30° N at 150 hPa (Fig. 7c). Such as at 220 hPa, northward advection on the western flank of the AMA between 20° E and 35° E is bringing polluted air to the Eastern Mediterranean UT. At the bottom of the LS (100 hPa, Fig. 6a), the CO distribution over Africa is also dominated by the AMA and the TEJ but the mean CO concentrations have decreased by ∼30 ppbv probably as a result of slow vertical uplift.

In this section, we have highlighted the main CO transport pathways in the African UT based on averaged assimilated CO and wind fields for the month of July 2006. Below 150 hPa, pollution in the African UT is mostly coming from African emissions and particularly BB in Southern Africa uplifted within the WAM region and advected southward by the winter Hadley cell. At and above 150 hPa, the distribution of CO over Africa is mainly driven by westward transport of polluted air masses uplifted to the UT over Asia to Northeast Africa around 25° N–35° N by the AMA and to the African Atlantic coast by the TEJ south of the AMA.

5 Variability of the CO transport pathways in the African UT

The dynamical processes responsible for the transport of CO between the Asian and the African UT that were described

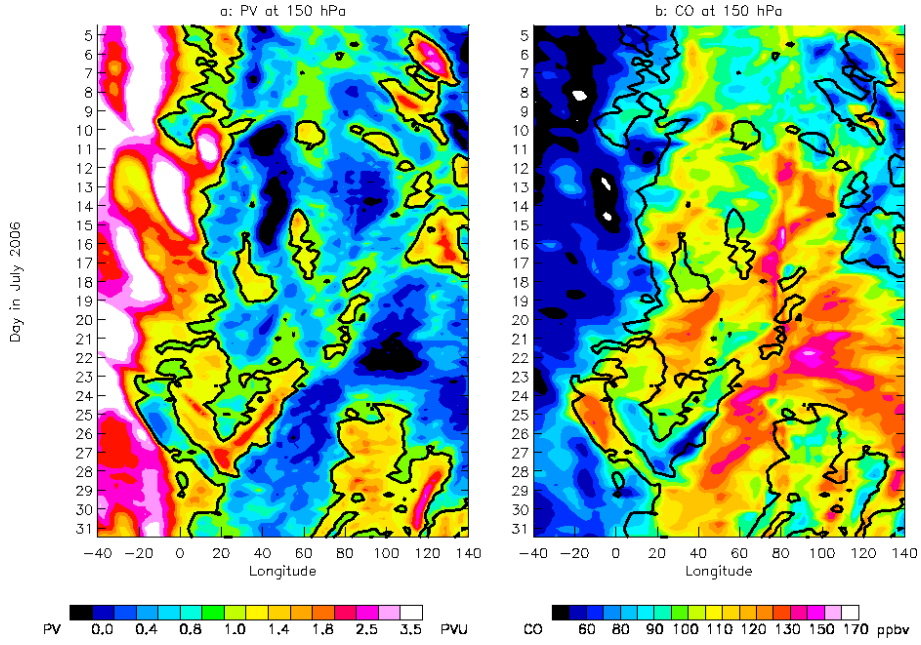

Fig. 8. Hovmoller diagrams of 6 h **(a)** PV and **(b)** CO assimilated mixing ratios at 150 hPa averaged over the latitudinal band 25° N–35° N for 5–31 July. The 1.2 PVU potential vorticity contour are represented as black solid lines.

in the previous section are subject to variations on synoptic timescales. One of the advantage of the assimilation of spaceborne observations is to provide 4-D fields with a synoptic timescale resolution not achievable with the observations alone. In this section, we take advantage of this property of the assimilated fields to study the impact of the variations of the TEJ and the AMA upon the distribution of CO in the African UT. The AMA is not a steady feature, it is subject to important variations on synoptic timescales. Based on meteorological data for the years 1987 to 1991, Popovic and Plumb (2001) have shown that the UT divergent flow in the Asian Monsoon area, present during the whole season varies greatly in strength and shape. In particular, eddy shedding and westward propagation of the anticyclone are the most dramatic changes observed. Based on the 4 years they have analyzed, they assess that eddy sheddings, that follow a strengthening and an elongation of the anticyclone by a couple of days, are occuring a few times per summer with a duration of 4 to 8 days. Air masses within the AMA are characterized by low PV values and Popovic and Plumb (2001) have used PV fields to determine the position and extension of the AMA and of the eddy sheddings and westward propagation events.

In order to evaluate the impact of such events upon the CO distribution in the UT, we display the Hovmoller diagrams of PV computed from the ECMWF analyses and of CO mixing ratios from the MOCAGE-MLS assimilation system averaged in the latitudinal band 25–35° N at 150 hPa (Fig. 8). We arbitrarily use a value of 1.2 PVU to delimit the AMA (black contour in Fig. 8). On average, the AMA extends westward to 20° E but it is subject to a strong variability as shown by the PV fields. From 5 to 16 July, the AMA is relatively stable and characterized by two main vortices centered at 50° E and 80° E. After 17 July, these two vortices weaken and the AMA is starting to strengthen again above Asia between 100° E and 120° E and to elongate until 24 July. The AMA then splits into two main vortices propagating westward (20–70° E) and eastward. Furthermore, between 23 and 27 July two small and weak vortices centered at 30° E and 10° W show up. Over the whole period, there is a clear anti-correlation between the CO concentrations (Fig. 8b) and the PV fields (Fig. 8a) with a correlation coefficient of −0.73. Within the 1.2 PVU contour, the CO mixing ratios are roughly larger than 90 ppbv. After the split of the AMA around 24 July, CO enhanced concentrations are found within the two main vortices and follow the same shoehorse shape than the PV contours. Between 23 and 27 July, enhanced CO concentrations are also found in the two weak westernmost vortices. At 100 hPa (not shown), Asian transient convective events are not perturbing the CO distribution and the strong anticyclonic circulation is the main dynamical process controlling the CO distribution resulting in correlation coefficient of −0.89 between the PV values and the CO concentrations. At the opposite, at 220 hPa (not shown) the correlation coefficient is reduced to −0.47 because the anticyclonic circulation is weaker and convection is more important than at 150 hPa. On the southern flank of the AMA, south of 25° N, the upper tropospheric circulation

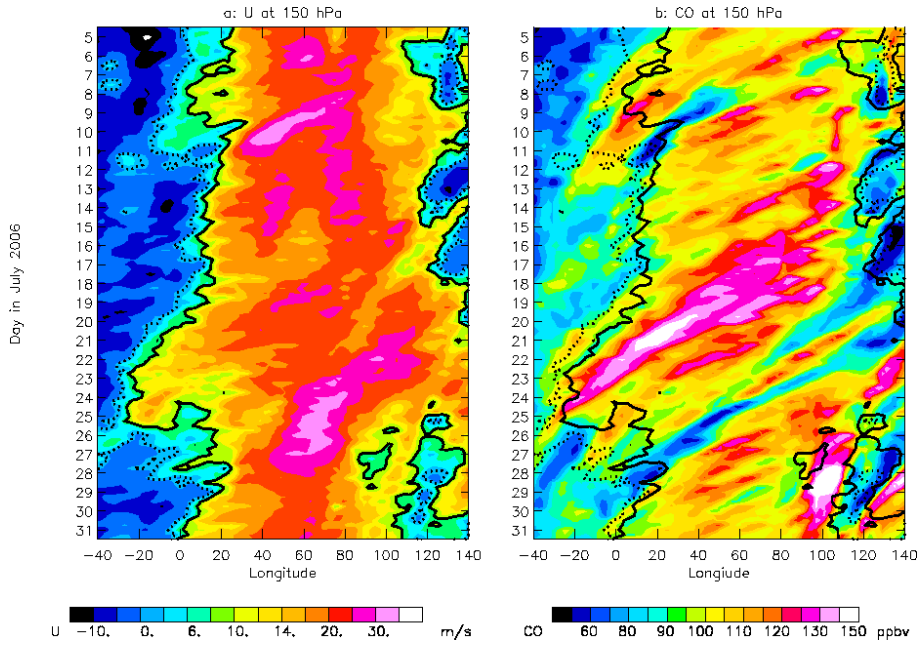

Fig. 9. Hovmoller diagrams of 6 h **(a)** zonal wind (greater than 0 for easterlies) and **(b)** CO assimilated mixing ratios at 150 hPa averaged over the latitudinal band 15° N–25° N for 5–31 July. Black solid lines: 10 m/s zonal wind, black dotted lines: 5 m/s zonal wind.

between Asia and Africa is controlled by westward transport by the TEJ (Fig. 7c). Therefore, to evaluate the impact of the variability in the strength of the TEJ upon the CO distribution, we display Hovmoller diagrams of zonal wind velocities from the ECMWF analyses and of CO mixing ratios from the MOCAGE-MLS assimilation system at 150 hPa averaged in the 15–25° N latitudinal band (Fig. 9). The TEJ is delimited by the 10 m/s contour of westward wind velocities (Black solid line). During most of 5–31 July, the TEJ is confined eastward of 10° E with the exception of 7–10 July and 21–26 July when the TEJ is reaching 0° E and 20° W respectively. In the same latitudinal band, the highest CO concentrations are mostly confined within the boundaries of the TEJ. The westward propagations of the TEJ on 7–11 July and 21–26 July are correlated with similar westward propagations of enriched CO air masses. The strong westward propagation of the TEJ on 21–26 July, weaker but noticeable at 220 hPa (not shown) is responsible for the sharp peak in CO concentrations between 20° N and 30° N detected by MOZAIC and reproduced by MOCAGE-MLS on 21 July (Fig. 5). For the same reasons than for the PV-CO relationship described above, the correlation coefficients between the zonal winds and the CO concentrations are increasing from 0.48 at 220 hPa to 0.61 at 100 hPa (not shown).

6 Conclusions

In order to study the main dynamical processes responsible for the transport of pollution in the African UT during NH summer, we have assimilated MLS UTLS CO observations in the MOCAGE CTM with the MOCAGE-PALM system and a 3-D-FGAT method. Prior to the assimilation, the MLS CO observations, known to be biased in the UTLS, have been adjusted towards a climatological tropical profile. Around the lowermost pressure level sampled by MLS (215 hPa), comparisons with the independent MOZAIC in situ observations have shown that the assimilation allows us to reproduce the CO UT distribution but also the in situ observations at high spatial and temporal resolution. The most important discrepancy is a high bias of ∼10 ppbv over Africa between 5° N and 20° N. The CO assimilated fields provided by the MOCAGE-MLS system have allowed us to establish the main transport pathways of CO in the African UT. Below 150 hPa, convective uplift of air masses impacted by BB in Southern Africa within the WAM region between 0° N and 12° N is the main contributor to the latitudinal CO maximum. Below ∼180 hPa, the polluted air masses deposited in the UT are vented mostly southward by the upper branch of the winter Hadley cell. At and above 150 hPa the main contributors are westward transport by the TEJ and the AMA of Asian polluted air masses that have been uplifted up to 100 hPa resulting in maxima CO concentrations over North Africa around 25° N. We took advantage of the synoptic timescale resolution of the MOCAGE-MLS assimilation

system to study the impact of the variability of the dynamical processes responsible for the interconnection between the Asian and African UT upon the CO distributions. In the UT (150 hPa) over Northern Africa (25° N–35° N), the variations of the AMA characterized by successive periods of elongations and sheddings generate variations of the CO concentrations by a factor of 2 between 60 and 120 ppbv. South of the AMA (15° N–25° N) TEJ westward propagation events are responsible for enhancements of the CO concentrations of up to 50 ppbv as far as the African Atlantic coast. This study has highlighted the strength of the assimilation of spaceborne chemical observations in a CTM to study transport processes in th UT. This first step has opened important perspectives. First, the assimilation of CO MLS observations on longer time periods will allow us to study the variability of the transport pathways in the African and Mediterranean UT on intraseasonal and seasonal timescales. A further step will also consist in assimilating O_3 MLS observations to evaluate the impact of the transport pathways upon the UT O_3. In particular, the CO-O_3 relationship established from assimilated fields will provide a powerful tool to discriminate the origin of the air masses.

Acknowledgements. B. Barret is funded by the European Commission within the AMMA programme. Based on a French initiative, AMMA was built by an international scientific group and is currently funded by a large number of agencies, especially from France, the United Kingdom, the United States, and Africa. It has been the beneficiary of a major financial contribution from the European Communities Sixth Framework Research Programme. The authors acknowledge for the strong support of the European Commission, Airbus, and the Airlines (Austrian-Airlines, Austrian, Air France) who carry free of charge the MOZAIC equipment and perform the maintenance since 1994. MOZAIC is presently funded by INSU-CNRS, Meteo-France, and FZJ (Forschungszentrum Julich, Germany). Costs of transport for the MOZAIC instrumentation onboard the Air Namibia aircraft in 2006 were paid by INSU-CNRS and by the Network of Excellence ACCENT; maintenance costs were paid by FZJ. Interpolated OLR data are provided by the NOAA/OAR/ESRL PSD, Boulder, Colorado, USA, from their Web site at http://www.cdc.noaa.gov.

Edited by: C. Reeves

References

Barret, B., Turquety, S., Hurtmans, D., Clerbaux, C., Hadji-Lazaro, J., Bey, I., Auvray, M., and P.-F. Coheur: Global carbon monoxide vertical distributions from spaceborne high-resolution FTIR nadir measurements, Atmos. Chem. Phys., 5, 2901–2914, 2005, http://www.atmos-chem-phys.net/5/2901/2005/.

Bechtold, P., Bazile, E., Guichard, F., Mascart, P., and Richard, E.: A mass flux convection scheme for regional and global models, Q. J. Roy. Meteor. Soc., 127, 869–886, 2001.

Bernath, P. F., McElroy, C. T., Abrams, M. C., et al.: Atmospheric Chemistry Experiment (ACE): Mission overview, Geophys. Res. Lett., 32, L15S01, doi:10.1029/2005GL022386, 2005.

Berthet, G., Esler, J. G., and Haynes, P. H.: A lagrangian perspective of the tropopause and the ventilation of the lowermost stratosphere, J. Geophys. Res., 112, D18102, doi:10.1029/2006JD008295, 2007.

Bousserez, N., Attie, J.-L., Peuch, V.-H., et al.: Evaluation of the MOCAGE chemistry transport model during the ICARTT/ITOP experiment, J. Geophys. Res., 112, D10S42, doi:10.1029/2006JD007595, 2007.

Buis, S., Piacentini, A., Declat, D., et al.: A Computational framework for assembling high performance computing applications, Concurrency Computat. Pract. Exper., 18, 247–262, 2006.

Chatfield, R. B., Guan, H., Thompson, A. M., and Witte, J. C., Convective lofting links Indian Ocean air pollution to paradoxical South atlantic ozone maxima, Geophys. Res. Lett., 31, L06103, doi:10.1029/2003GL018866, 2004.

Clerbaux, C., George, M., Turquety, S., Walker, K. A., Barret, B., Bernath, P., Boone, C., Borsdorff, T., Cammas, J. P., Catoire, V., Coffey, M., Coheur, P.-F., Deeter, M., De Mazire, M., Drummond, J., Duchatelet, P., Dupuy, E., de Zafra, R., Eddounia, F., Edwards, D. P., Emmons, L., Funke, B., Gille, J., Griffith, D. W. T., Hannigan, J., Hase, F., Hpfner, M., Jones, N., Kagawa, A., Kasai, Y., Kramer, I., Le Flochmon, E., Livesey, N. J., Lpez-Puertas, M., Luo, M., Mahieu, E., Murtagh, D., Ndlec, P., Pazmino, A., Pumphrey, H., Ricaud, P., Rinsland, C. P., Robert, C., Schneider, M., Senten, C., Stiller, G., Strandberg, A., Strong, K., Sussmann, R., Thouret, V., Urban, J., and Wiacek, A.: CO measurements from the ACE-FTS satellite instrument: data analysis and validation using ground-based, airborne and spaceborne observations, Atmos. Chem. Phys., 8, 2569–2594, 2008, http://www.atmos-chem-phys.net/8/2569/2008/.

Daniel, J. S. and Solomon, S.: On the climate forcing of carbon monoxide, J. Geophys. Res., 103, 13 249–13 260, 1998.

Deeter, M. N., Emmons L. K., Francis G. L., et al.: Operational carbon monoxide retrieval algorithm and selected results for the MOPITT instrument, J. Geophys. Res., 108, 4399, doi:10.1029/2002JD003186, 2003.

Dentener, F., Stevenson, D., Cofala, J., et al.: The impact of air pollutant and methane emission controls on tropospheric ozone and radiative forcing: CTM calculations for the period 1990–2030 , Atmos. Chem. Phys., 5, 1731–1755, 2005, http://www.atmos-chem-phys.net/5/1731/2005/.

Duncan, B. N. and Bey, I.: A modeling study of export pathways of pollution from Europe: Seasonal and Interannual variations (1987–1997), J. Geophys. Res., 109, D08301, doi:10.1029/2003JD004079, 2004.

Filipiak, M. J., Harwood, R. S., Jiang, J. H., Li, Q., Livesey, N. J., Manney, G. L., Read, W. G., Schwartz, M. J., Waters, J. W., and Wu, D. L.: Carbon Monoxide Measured by the EOS Microwave Limb Sounder on Aura: First Results, Geophys. Res. Lett., 32, L14825, doi:10.1029/2005GL022765, 2005.

Fisher, M. and Andersson, E.: Developments in 4D-Var and Kalman Filtering, ECMWF Technical Memoranda, 347, 1–36, 2001.

Folkins, I., Bernath, P., Boone, C., Donner, L. J., Eldering, A., Lesins, G., Martin, R. V., Sinnhuber, B.-M., and Walker, K.: Testing convective parameterizations with tropical measurements of HNO3, CO, H2O, and O3: Implications for the water vapor budget, J. Geophys. Res., 111, D23304, doi:10.1029/2006JD007325, 2006.

Folkins, I., Bernath, P., Boone, C., Lesins, G., Livesey, N., Thomp-

son, Walker, K., and Witte, J., Seasonal cycles of O3, CO, and convective outflow at the tropical tropopause, Geophys. Res. Lett., 33, L16802, doi:10.1029/2006GL026602, 2006.

Fu, R., Hu, Y., Wright, J. S., et al.: Short circuit of water vapor and polluted air to the global stratosphere by convective transport over the Tibetan Plateau (2006), Proc. Natl. Acad. Sci. USA., 103, 5664–5669, 2006.

Fu, T. M., Jacob, D. J., Palmer, P. I, et al.: Space-based formaldehyde measurements as constraints on volatile organic compound emissions in east and south Asia and implications for ozone (2007), J. Geophys. Res., 112, D06312, doi:10.1029/2006JD007853, 2007.

Geer, A. J., Lahoz, W. A., Bekki, S., et al.: The ASSET intercomparison of ozone analyses: method and first results, Atmos. Chem. Phys., 6, 5445–5474, 2006, http://www.atmos-chem-phys.net/6/5445/2006/.

Holloway, T., Levy, H., and Kasibhatla, P.: Global distribution of carbon monoxide, J. Geophys. Res., 105, D10, 12 123–12 147, 2000.

Hoskins, B. J. and Rodwell, M. J.: A model of the Asian summer monsoon. Part I: the global scale, J. Atmos. Sci., 52, 1329–1340, 1995.

Josse, B., Simon, P., and Peuch, V.-H.: Radon global simulations with the multiscale chemistry transport model MOCAGE, Tellus B, 56, 339–356, 2004.

Lamarque, J. F., Khattatov, B., Yudin, V., et al.: Application of a bias estimator for the improved assimilation of Measurements of Pollution in the Troposphere (MOPITT) carbon monoxide retrievals, J. Geophys. Res., 109, D16304, doi:10.1029/2003JD004466, 2004.

Lefevre, F., Brasseur, G. P., Folkins, I., Smith, A. K., and Simon, P.: Chemistry of the 1991–1992 stratospheric winter: threedimensional model simulations, J. Geophys. Res., 99, 8183–8195, 1994.

Lelieveld, J., Berresheim, H., Borrmann, S., et al.: Global Air Pollution Crossroads over the Mediterranean, Science, 298, 794–799, 2002.

Li, Q. L., Jacob, D. J., Logan, J. A., et al.: A Tropospheric Ozone Maximum Over the Middle East, Geophys. Res. Lett., 28(D17), 3235–3238, 2001.

Li, Q. L., Jiang, J. H., Wu, D. L., et al.: Convective outflow of South Asian pollution: A global CTM simulation compared with EOS MLS observations, Geophys. Res. Lett., 32, L14826, doi:10.1029/2005GL022762, 2005.

Liang, Q., Jaegle, L., Hudman R. C., et al.: Summertime influence of Asian pollution in the free troposphere over North America, J. Geophys. Res., D12S11, doi:10.1029/2006JD007919, 2007.

Livesey, N. J., Filipiak, M. J., Froidevaux, L., et al.: Validation of Aura Microwave Limb Sounder O_3 and CO observations in the upper troposphere and lower stratosphere, J. Geophys. Res., 113, D15S02, doi:10.1029/2007JD008805, 2008.

Louis, J.-F.: A parametric model of vertical eddy-fluxes in the atmosphere, Bound. Lay. Meteor., 17, 187–202, 1979.

Mari, C. H., Cailley, G., Corre, L., et al.: Tracing biomass burning plumes from the Southern Hemisphere during the AMMA 2006 wet season experiment, Atmos. Chem. Phys. Discuss., 7, 17 339–17 366, 2007.

Mari, C. and Prospero, J., African Monsoon Multidisciplinary Analysis-Atmospheric Chemistry (AMMA-AC): a new IGAC task; IGACtivities Newsletter, 31, 2–13, 2005.

Massart, S., Cariolle, C., and Peuch, V.-H., Towards an improvement of the atmospheric ozone distribution and variability by assimilation of satellite data, C. R. Geosciences, 15, 1305–1310, 2005.

Massart, S., Piacentini A., Cariolle, D., El Amraoui, L., and Semane N., Assessment of the quality of the ozone measurements from the Odin/SMR instrument using data assimilation, Can. J. Phys., 85, 1209–1223, 2007.

McMillan, M. W., Barnet, C., Strow, L., et al.: Daily global maps of carbon monoxide from NASAs Atmospheric Infrared Sounder, Geophys. Res. Lett., 32, L11801, doi:10.1029/2004GL021821, 2005.

Nedelec, P., Cammas, J.-P., Thouret, V., et al.: An improved infrared carbon monoxide analyser for routine measurements aboard commercial Airbus aircraft: technical validation and first scientific results of the MOZAIC III programme, Atmos. Chem. Phys., 3, 1551–1564, 2003, http://www.atmos-chem-phys.net/3/1551/2003/.

Pradier, S., Attie, J.-L., Chong, M., et al.: Evaluation of 2001 springtime CO transport over West Africa using MOPITT CO measurements assimilated in a global chemistry transport model, Tellus B, 58, 163–176, 2006.

Park, M., Randel, W. J., Gettelman, A., Massie, S. T., and Jiang, J. H.: Transport above the Asian summer monsoon anticyclone inferred from Aura Microwave Limb Sounder tracers, J. Geophys. Res., 112, D16309, doi:10.1029/2006JD008294, 2007.

Popovic, J. and Plumb, R. A.: Eddy Sheding from the Upper-Tropospheric Asian Monsoon Anticyclone, J. Atmos. Sci., 58, 93–104, 2001.

Pumphrey, H. C., Filipiak, M. J., Livesey, N. J., et al.: Validation of middle-atmosphere carbon monoxide retrievals from MLS on Aura, J. Geophys. Res., 112, D24S38, doi:10.1029/2007JD008723, 2007.

Randel, W. J. and Park, M.: Deep convective influence on the Asian summer monsoon anticyclone and associated tracer variability observed with Atmospheric Infrared Sounder (AIRS), J. Geophys. Res., 111, D12314, doi:10.1029/2005JD006490, 2006.

Raspollini, P., Belotti, C., Burgess A., et al.: MIPAS level 2 operational analysis, Atmos. Chem. Phys., 6, 5605–5630, 2006, http://www.atmos-chem-phys.net/6/5605/2006/.

Redelsperger, J. L., Thorncroft, C. D., Diedhiou, A., et al.: African monsoon multidisciplinary analysis – An international research project and field campaign, Bull. Amer. Soc., 87, 1739, doi:10.1175/BAMS-87-12-1739, 2006.

Ricaud P., Barret, B., Attie, J.-L., et al.: Impact of land convection on troposphere-stratosphere exchange in the tropics, Atmos. Chem. Phys., 7, 5639–5657, 2007, http://www.atmos-chem-phys.net/7/5639/2007/.

Richter A., Burrows, J. P., Nuss, H., et al.: Increase in tropospheric nitrogen dioxide over China observed from space, Nature, 437, 129–132, 2005.

Rinsland, C. P., Luo, M., Logan, J. A., et al.: Nadir Measurements of carbon monoxide distributions by the Tropospheric Emission Spectrometer onboard the Aura Spacecraft: Overview of analysis approach and examples of initial results, Geophys. Res. Lett., 33, L22806, doi:10.1029/2006GL027000, 2006.

Sathiyamoorthy, V., Pal, P. K., and Joshi, P. C.: Intraseasonal variability of the Tropical Easterly Jet, Meteorol. Atmos. Phys., 96,

305–316, 2007.

Saunois M., Mari, C., Thouret V., et al.: An idealized two-dimensional approach to study the impact of the West African monsoon on the 2 meridional gradient of tropospheric ozone, J. Geophys. Res., 113, D07306, doi:10.1029/2007JD008707, 2008.

Sauvage, B., Thouret, V., Cammas, J. P., Gheusi, F., Athier, G., and Nedelec, P.: Tropospheric ozone over Equatorial Africa: regional aspects from the MOZAIC data, Atmos. Chem. Phys., 5, 311–335, 2005,
http://www.atmos-chem-phys.net/5/311/2005/.

Sauvage, B., Thouret, V., Cammas, J.-P., Brioude, J., Nedelec, P., and Mari, C.: Meridional ozone gradients in the African upper troposphere, Geophys. Res. Lett., 34, L03817, doi:10.1029/2006GL028542, 2007.

Sauvage, B., Gheusi, F., Thouret, V., Cammas, J.-P., Duron, J., Escobar, J., Mari, C., Mascart, P., and Pont, V.: Medium-range mid-tropospheric transport of ozone and precursors over Africa: two numerical case studies in dry and wet seasons, Atmos. Chem. Phys., 7, 5357–5370, 2007,
http://www.atmos-chem-phys.net/7/5357/2007/.

Scheeren, H. A., Lelieveld, J., Roelofs, G. J., et al.: The impact of monsoon outflow from India and Southeast Asia in the upper troposphere over the eastern Mediterranean, Atmos. Chem. Phys., 3, 1589–1608, 2003,
http://www.atmos-chem-phys.net/3/1589/2003/.

Shindell, D. T., Faluvegi, G., Stevenson, D. S., et al.: Multi-model simulations of carbon monoxide: Comparison with observations and projected near-future changes, J. Geophys. Res., 111, D19306, doi:10.1029/2006JD007100, 2006.

Stockwell, W. R., Kirchner, F., Khun, M., and Seefeld, S.: A new mechanism for regional atmospheric chemistry modelling, J. Geophys. Res., 102, 25 847–25 879, 1997.

Stavrakou, T. and Muller, J.-F.: Grid-based versus big region approach for inverting CO emissions using Measurement of Pollution in the Troposphere (MOPITT) data, J. Geophys. Res., 111, D15304, doi:10.1029/2005JD006896, 2006.

Stohl, A., Eckhardt, S., Forster, C., James, P., and Spichtinger, N.: On the pathways and timescales of intercontinental air pollution transport, J. Geophys. Res., 107, 4684, doi:10.1029/2001JD001396, 2002.

Teyssedre, H., Michou, M., Clark, H. L., et al.: A new tropospheric and stratospheric Chemistry and Transport Model MOCAGE-Climat for multi-year studies: evaluation of the present-day climatology and sensitivity to surface processes, Atmos. Chem. Phys., 7, 5815–5860, 2007,
http://www.atmos-chem-phys.net/7/5815/2007/.

Thompson, A. M.: The Oxidizing Capacity of the Earths Atmosphere: Probable Past and Future Changes, Science, 256, 1157–1165, 1992.

Waters, J. W., Froidevaux, L., Harwood, R. S., et al.: The Earth Observing System Microwave Limb Sounder (EOS MLS) on the Aura satellite, IEEE Trans. Geosci. Remote Sens., 44, 1075–1092, 2006.

Weaver, A. and Courtier, P.: Correlation modelling on the sphere using a generalized diffusion equation, Q. J. Roy. Meteorol. Soc., 127, 1815–1846, 2001.

Yudin, V. A., Petron, G., Lamarque, J. F., et al.: Assimilation of the 2000–2001 CO MOPITT retrievals with optimized surface emissions, Geophys. Res. Lett., 31, L20105, doi:10.1029/2004GL021037, 2004.